# Small-Cell Wireless Backhauling

## A Non-Line-of-Sight Approach for Point-to-Point Microwave Links

M. Coldrey*, H. Koorapaty**, J.-E. Berg***, Z. Ghebretensaé***, J. Hansryd****, A. Derneryd*, S. Falahati***
*Ericsson Research, Ericsson AB, Gothenburg, Sweden
**Ericsson Research, Ericsson Inc, San Jose, USA
***Ericsson Research, Ericsson AB, Kista, Sweden
****System & Technologies, PDU Microwave, Ericsson AB, Mölndal, Sweden

*Abstract*—**In this paper we investigate the feasibility of using microwave frequencies for fixed non-line-of-sight wireless backhauling connecting small-cell radio base stations with an aggregation node in an outdoor urban environment, i.e. a typical heterogeneous network scenario. We study system level simulations for a point-to-point system where the wave propagation is based on diffraction over rooftops. We further investigate the effects of carrier frequency, interference, antenna height, rain, and tolerance to antenna alignment errors. It is found that the higher frequencies offer not only larger bandwidths but also higher antenna gains which would ideally work to their advantage. However, these advantages may be lost when taking antenna alignment errors and rain into account. Different frequencies simply have their different trade-offs.**

***Keywords: Wireless backhaul, heterogenous networks, HetNet, small-cell, diffraction, microwaves, millimeterwaves, non-line-of-sight, point-to-point***

## I. INTRODUCTION

A general consensus within the wireless industry today is that the capacity offered in existing cellular radio access networks based on macro cells cannot fulfill the requirements from future mobile broadband services unless a capacity boost is achieved at specific locations such as hotspots, cell edges and indoor locations. One approach to increase the capacity at these locations is to deploy low power (e.g., pico) radio base stations (RBSs) covering smaller cells within the macro cell coverage area, i.e. a heterogeneous network [1], [2]. Assuming that each macro cell is supported by a few small cells, the number of cells in the network and thus the required number of mobile backhaul (MBH) links will increase dramatically. Due to its small coverage area it will be important that the small-cell pico RBS is placed in a correct location, not limited by the availability of a broadband connection for MBH. Further, the pico RBS will in many cases be placed in the clutter, below rooftop level, preventing a clear Line-Of-Sight (LOS) between the pico RBS and the aggregation node that is co-located with the macro RBS above rooftop. Traditional MBH technologies such as copper, optical fiber or LOS microwave links may thus not always fit such a heterogeneous backhaul scenario and they need to be complemented by low cost wireless Non-Line-Of-Sight (NLOS) MBH links. NLOS propagation has traditionally been proposed only for carrier frequencies below 6 GHz. However, wideband spectrum on these frequencies is a scarce resource and if made available it is also very attractive to use it for mobile broadband services in the radio access network.

Traditional fixed service LOS microwave point-to-point (PtP) links operate in licensed frequency bands between 6 GHz and 42 GHz on channel bandwidths ranging from 3.5 MHz up to 112 MHz. Due to the nature of the traffic carried by the MBH, traditional PtP LOS links are required to have high availability (e.g., 5 9's). One can however question what kind of availability requirements one can and should expect for NLOS backhauling. High availability is something one has to trade off when moving a LOS link into the clutter. However, if the small-cell anyway is within the coverage area of a macro cell then it might be feasible with relaxed availability requirements. The requirement on small-cell MBH is becoming an increasingly important topic that is discussed within the industry and academia and it is driven by the evolution towards flexible and cost effective heterogeneous deployments.

Over the last few years, there has also been an increased interest in the higher frequency bands especially the 60 GHz band (9 GHz of bandwidth between 57–66 GHz) and the 70/80 GHz band (total 10 GHz bandwidth between 71–86 GHz) for MBH applications. Compared to the 56 and 112 MHz channels available for traditional microwave links, the bandwidths offered by these bands are very large which make them attractive. Parts of the 60 GHz band is license free spectrum which means that anyone can deploy systems within that band as long as the equipment complies with regulations. Nevertheless, this frequency is especially interesting for small-cell MBH applications since the excess oxygen loss at this band may attenuate interference from neighboring links enabling efficient frequency re-use (given of course that the overall path loss is not too high). The licensing of 70/80 GHz varies from country to country. It is either light licensing (e.g., in USA, UK) or full licensing (e.g., Germany, Ireland). An overview of microwave link technologies is found in, e.g., [3].

In this work we present results showing the feasibility of using frequency bands above 6 GHz for heterogeneous MBH links. We compare the results with the expected performance of a NLOS MBH link in the 2.3 GHz band. We study an urban heterogeneous deployment scenario where macro RBSs are located above rooftop and the pico RBSs are located on building walls below rooftop. The signal propagation between MBH hub antennas located at the macro RBS and MBH remote antennas located at the pico RBS is based on knife-edge diffraction over rooftops. We provide system level simulations for a PtP system and we study the effects of carrier frequency,

978-1-4673-1881-5/12/$31.00 ©2012 IEEE

interference, antenna height, rain attenuation, oxygen absorption at 60 GHz, and antenna alignment errors.

## II. System Model

### A. NLOS propagation model

The path loss used in our simulations is based on a multiple (knife-edge) diffraction model over buildings, as shown in Figure 1, where the diffraction calculations are based on Fresnel-Kirchhoff integrals [4]. All obstructing buildings along the signal path are considered where each building is modeled with multiple diffraction shields. In principle, the higher the frequency, the less impact the buildings have on the overall diffraction loss since the first Fresnel zone becomes smaller for higher frequencies. Thus, the lower frequencies are more subject to multiple diffractions. The hub antenna is always located above rooftop level, $h_1 > 0$ m, and the remote antenna (i.e., the small-cell antenna) is at rooftop level, $h_2 = 0$ m, or below, $h_2 > 0$ m. When the remote antenna is lowered from LOS level down towards the street level the building in front of the remote antenna causes the greater part of the increased path loss. The shorter the distance $D$ is, the higher the path loss becomes in NLOS conditions.

Only the diffracted ray is considered when calculating the path loss for the desired link. This means that a remote antenna with narrow beam should be pointing towards the main diffraction point in order to maximize received signal strength. In reality there often exist some reflected rays and it could be so that the received signal strength is higher when the remote antenna is pointed towards a reflected ray instead of the diffracted ray. The diffracted ray, however, always exists in a more or less known direction while a reflected ray is not always present and it is difficult to know in advance which direction it is coming from. Reflected rays are considered in a simplified manner when the path loss is determined for interfering links located in the rear direction of the remote antenna. It is then assumed that a reflection occurs in the building in front of the remote antenna for interferers located in the rear direction. The result is that in NLOS the received interfering signals (i.e., signals from other links) always arrive in the main or side lobe direction of the remote antenna and not in the back lobe direction.

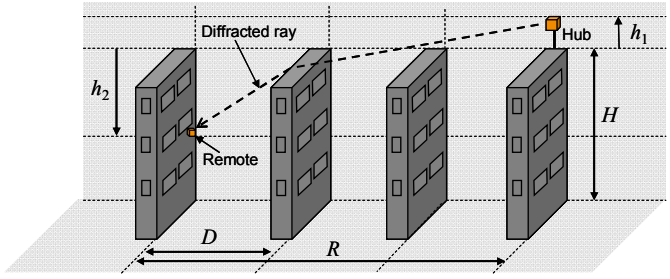


Figure 1: Scenario for path loss model with diffracted ray over buildings. Together with frequency and antenna sizes, $H$, $R$, $D$, $h_1$, and $h_2$ are parameters used in the model.

### B. Antenna model

The antenna model used in this work is a single pencil beam generated by a circular aperture. The antenna radiation pattern model is created from the ETSI requirements on LOS radio link equipment [5] and the radiation pattern envelope is combined with a Gaussian beam shape suitable for the studied frequency band from 2.3 to 73 GHz.

### C. Urban deployment scenario

We investigate the system performance in an urban deployment scenario, as depicted in Figure 1, where the heights of all buildings are assumed to be $H$ = 28 m and all street widths $D$ = 15 m. The remote antenna distance below rooftop is either fixed to a default value of $h_2$ = 20 m or is in some examples varied while the hub antenna is always located $h_1$ = 5 m above rooftop. Figure 2 shows the number of remotes assigned to each MBH hub. In this example we have in total 11 hubs and 27 remotes where the remote to hub association is based on minimum path loss. The hop lengths vary between 46 and 450 m, with a median hop length of 175 m. Macro (or hub) locations have been taken from a real urban macro network deployment in Stockholm, Sweden, and the remote or pico locations (e.g., hot spots) have been added synthetically.

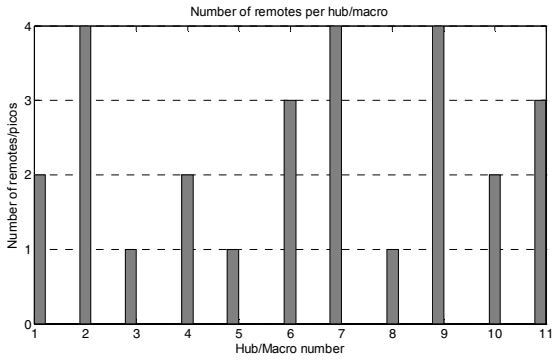


Figure 2: Pico assignment distribution in an urban deployment

### D. NLOS PtP backhaul link model

In the NLOS PtP backhaul link model it is assumed that each individual link has its own antennas that are aligned towards a diffraction point. When calculating the link gain using our propagation model we also include the effects of rain, oxygen absorption (for 60 GHz), and antenna misalignment. The receiver noise is assumed to consist of thermal noise and a noise figure of 3 dB. Once the link gains (excl. transmit powers) for all links have been determined, we calculate the required transmit powers where the transmit power for each link is chosen such that a receiver Signal-to-Noise Ratio (SNR) target of 30 dB is fulfilled with a margin. We use a 5 dB margin which includes a fading and implementation margin where the implementation margin consists of transmitter/receiver implementation imperfections such as, e.g., channel estimation errors, EVM, phase noise, etc. However, there is a maximum output power constraint which means that links might not fulfill the SNR target with the required margin. Once the transmit powers have been determined, we calculate the Signal-to-Interference and Noise Ratio (SINR) by including the interference that different links cause to each other. It is assumed that all links operate at the same frequency which is a worst case in terms of interference. Finally, the SINR values are mapped to data rates via scaling the Shannon capacity by the channel bandwidth. Since we have accounted for a fading and implementation margin of 5 dB, the calculated data rate is

maintained as long as not more than 5 dB in signal strength is lost over the link.

## III. Simulation Results

In this section we provide results from PtP simulations for systems operating at 2.3, 10, 24, 60, and 73 GHz. The 2.3 GHz carrier is chosen for comparing the performance of the microwave links with traditional NLOS sub 6 GHz links. To have a fair comparison, we assume (with exception for the case study) that all frequencies use the same bandwidth of 28 MHz, same maximum output power of 30 dBm, and same antenna sizes. We realize that output powers and channel bandwidths will in practice vary between different carrier frequencies and a case study investigating performance with different bandwidths and output powers is presented in Section III.E. The deployment scenario is described in Section II.C and, unless otherwise stated, it is assumed that there is no rain, perfectly aligned antennas, and frequency reuse one. The simulation results are presented as cumulative distribution functions (C.D.F.) over SINR and data rate. Due to space limitations we present only downlink (hub to remote) results. Finally, the antenna sizes are fixed to be relatively small where the hub antenna diameter is assumed to be 200 mm and the remote antenna diameter 100 mm. The lower frequencies would of course benefit from using larger antennas, but the antenna sizes are intentionally kept small to guarantee a low visual impact. The corresponding antenna gains and beamwidths are given in Table I.

Table I: Antenna gain and beamwidth for the selected frequencies and antenna sizes

| Frequency (GHz) | 100 mm diameter | | 200 mm diameter | |
|---|---|---|---|---|
| | Gain (dBi) | Beamwidth (deg) | Gain (dBi) | Beamwidth (deg) |
| 2.3 | 6 | 87 | 12 | 43 |
| 10 | 19 | 20 | 25 | 10 |
| 24 | 26 | 8.3 | 32 | 4.1 |
| 60 | 34 | 3.3 | 40 | 1.7 |
| 73 | 36 | 2.7 | 42 | 1.4 |

### A. Interference penalty

In Figure 3 the SNR and SINR are shown for the different frequencies. We notice that the lower frequencies (2.3 and 10 GHz) exhibit more penalty than the higher frequencies. For fixed antenna sizes, the lower frequencies have wider beamwidths than the higher frequencies (see Table I) and thus cause more spatial interference. Many of the high frequency links are in principle interference-free and reach also the maximum SNR of 35 dB which equals the chosen SNR target of 30 dB plus a fading and implementation margin of 5 dB.

### B. Rain attenuation

Here we study the effect of intensive 50 mm/hour rain on SINR and data rate. Figure 4 shows the SINR penalty when it rains compared to no rain. We see that the lower frequencies do not suffer much (if any) from rain attenuation while the higher frequencies show penalties in the order of a few dB. The corresponding data rates are shown in Figure 5 and we see that many of the high frequency links reach the maximum data rate. Overall, the rain attenuation is small due to the relatively short hop lengths in our chosen deployment scenario. Furthermore, the rain does not only attenuate the desired signal but also all the interfering signals. Finally, we can also observe that the 60 GHz system, due to the excess oxygen absorption loss, shows larger maximum penalties than the 73 GHz system.

### C. Antenna misalignment

In this example we introduce random antenna alignment errors (AAEs) at all antennas and we model the AAE as Normal distributed with zero mean and unit standard deviation (in degrees). The AAE is limited to ±3 degrees. Figure 6 shows the effect of AAE on SINR and Figure 7 shows the corresponding data rates. It is very noticeable how the higher frequencies due to narrower antenna beamwidths become much more sensitive to AAEs, thus, making it important to have robust antenna installations and good alignment methods that can handle the alignment sensitivity. The 24 GHz system shows a nice compromise between antenna gain and robustness to AAE.

### D. Varying remote antenna height

Here we study the performance when the remote antenna is lowered from rooftop level (LOS) to 5 m below rooftop and finally to 20 m below rooftop. Figure 8 shows the SINR for different remote antenna heights and Figure 9 shows the corresponding data rates. We observe a loss in SINR and data rate when moving the pico antenna towards the street level. However the losses are moderate due to interference limitation. That is, the interfering power is reduced along with the desired power. Figure 10 instead shows the SNR (interference-free) and here we clearly see, especially for the lower frequencies, the penalty when moving down the remote closer to the street level. This penalty is more dominant for the lower frequencies since the higher frequencies have (thanks to larger antenna gain) in LOS reached the maximum SNR of 35 dB (SNR target of 30 dB plus the 5 dB margin) without having to utilize the maximum output power. In other words, the high frequency links have some margin in the output power and this margin can to some extent be used to compensate for the additional path loss when moving the remote antenna deeper into NLOS. The lower frequency links do not have such margins to the same extent.

### E. Case study

In this section we provide results from a PtP case study with frequencies and respective bandwidths and transmit powers given in Table II. These parameters represent different cases that may arise from, e.g., practical constraints and different regulations in different regions. Figure 11 shows the data rates for the different systems in a non-ideal scenario with both 50 mm/hour rain and AAEs. In the ideal scenario with no rain and perfectly aligned antennas we see that the 73 GHz system outperforms all other systems thanks to its wide 250 MHz bandwidth. It is not as spectral efficient (in bps/Hz) as the other systems but bandwidth simply rules when it comes to pure data rate. However, with intensive rain and AEA the performance of the 73 GHz system quickly drops and the 24 GHz system shows better (and more robust) performance for at least 50% of the links.

TABLE II: SYSTEM PARAMETERS FOR CASE STUDY

| Frequency (GHz) | Channel bandwidth (MHz) | Max transmit power (dBm) |
|---|---|---|
| 2.3 | 20 | 40 |
| 10 | 28 | 23 |
| 24 | 50 | 21 |
| 60 | 50 | 10 |
| 73 | 250 | 10 |

## IV. CONCLUSIONS

We have investigated the feasibility of using microwave frequencies for NLOS small-cell backhauling in a heterogeneous network scenario. The wave propagation was based on diffraction over rooftops and we provided system simulation results for different frequencies (2.3, 10, 24, 60, and 73 GHz), bandwidths, and output powers. Overall, the higher frequencies showed best performance in ideal scenarios with no rain or antenna alignment errors, while the lower frequencies (2.3 GHz and to some extent 10 GHz) did not perform that well. The increased performance when going up in frequency is, for fixed antenna sizes, explained by the large increase in antenna gain and narrower beamwidths which also decreases the interference by spatial filtering. The lower frequencies would of course benefit a lot from using larger antennas, but the antenna sizes were intentionally kept small to guarantee a low visual impact. However, high-gain antennas make the system sensitive to antenna alignment errors which make the antenna installation procedure much more complicated. The higher frequencies may also offer more bandwidth which of course makes them attractive. But again this has to be traded off against increased rain attenuation (and oxygen absorption at 60 GHz) and antenna alignment complications. An acceptable compromise between the sub-6 GHz bands and the mm-wave bands at 60 GHz and higher could be mid-range bands from 15 GHz up to 30 GHz.

## REFERENCES


[1] A. Damnjanovic et al. "A survey on 3GPP heterogeneous networks". *IEEE Trans. on Wireless Communications*, vol.18, no.3, pp.10-21, June 2011.

[2] S. Landström, H. Murai, A. Simonsson, "Deployment Aspects of LTE Pico Nodes". In *Proc. IEEE International Conference on Communications (ICC 2011)*, June 2011.

[3] J. Hansryd and J. Edstam, "Microwave capacity evolution", *In Ericsson Review Journal*, no. 1, 2011, available online on www.ericsson.com.

[4] Grant R. Fowles, *Introduction to Modern Optics*, 2nd edition, Holt, Rinehart and Winston, Inc., New York, 1975.

[5] ETSI EN 302 217-4-2, "Fixed Radio Systems; Characteristics and requirements for point-to-point equipment and antennas; Part 4-2: Antennas", v1.5.1, 2010-01.


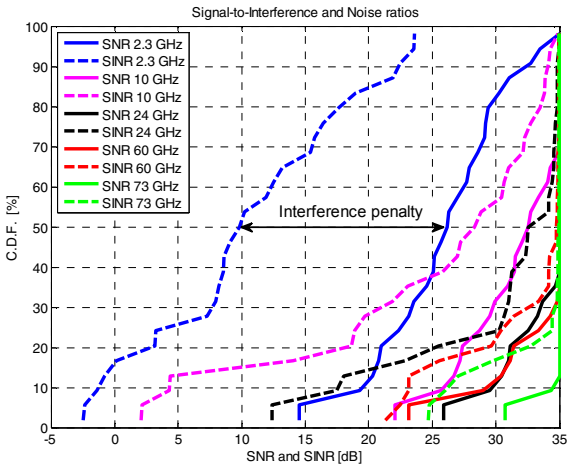


Figure 3: Interference penalty for different frequencies. The penalty is represented by the difference between SNR and SINR.

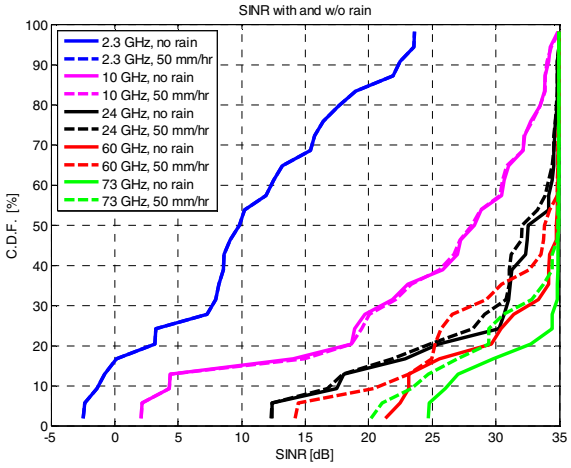


Figure 4: Rain attenuation penalty vs. SINR for different frequencies. The two blue curves are on top of each other.

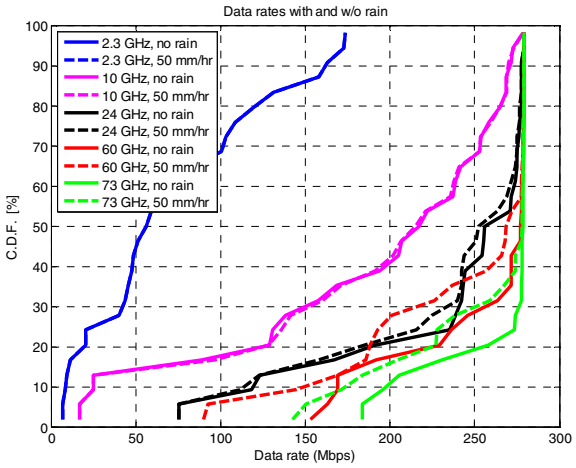


Figure 5: Rain attenuation penalty vs. data rate for different frequencies. The two blue curves are on top of each other.

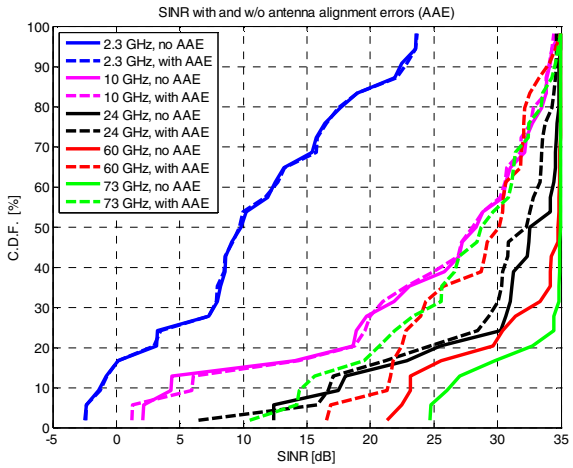


Figure 6: Antenna misalignment penalty vs. SINR for different frequencies. The two blue curves are on top of each other.

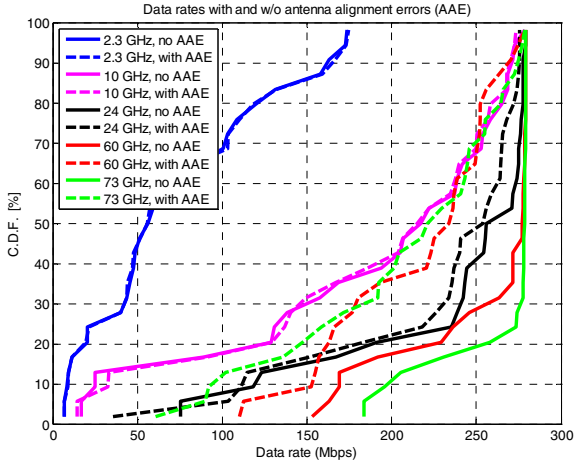


Figure 7: Antenna misalignment penalty vs. data rate for different frequencies. The two blue curves are on top of each other.

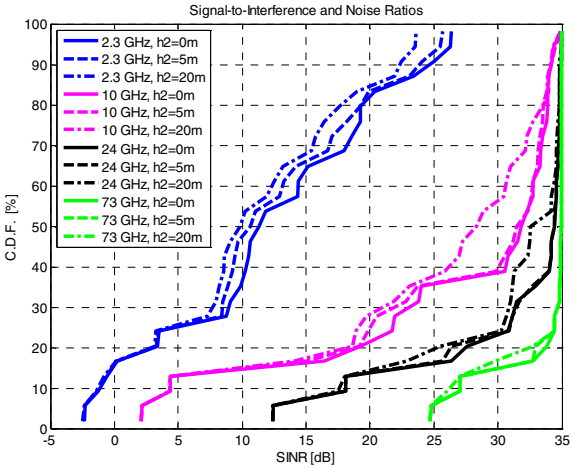


Figure 8: SINR for varying remote antenna height $h_2$ = 0, 5, 20 m and for different frequencies.

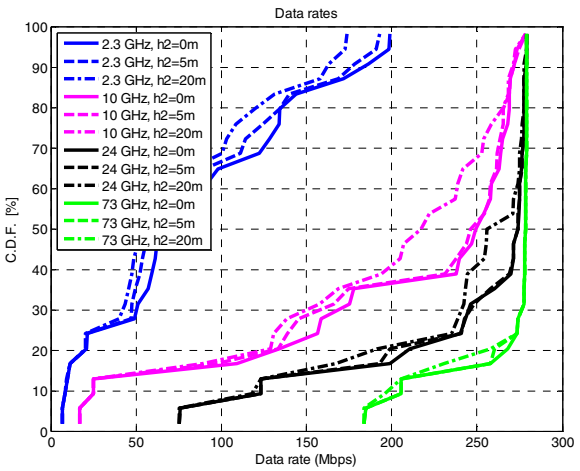


Figure 9: Data rate for varying remote antenna height $h_2$ = 0, 5, 20 m and for different frequencies.

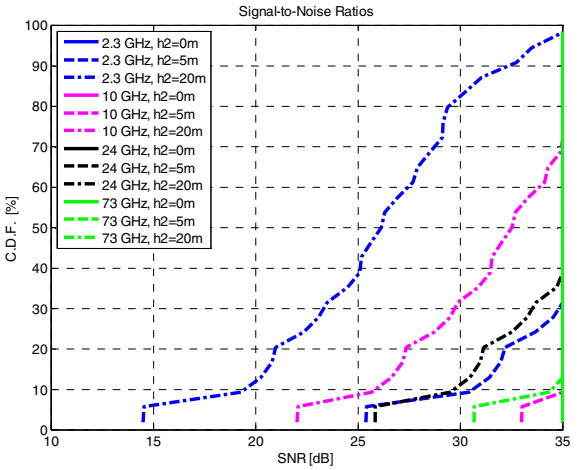


Figure 10: SNR (interference free) for varying remote antenna height $h_2$ = 0, 5, 20 m and for different frequencies. All solid curves are on top of each other.

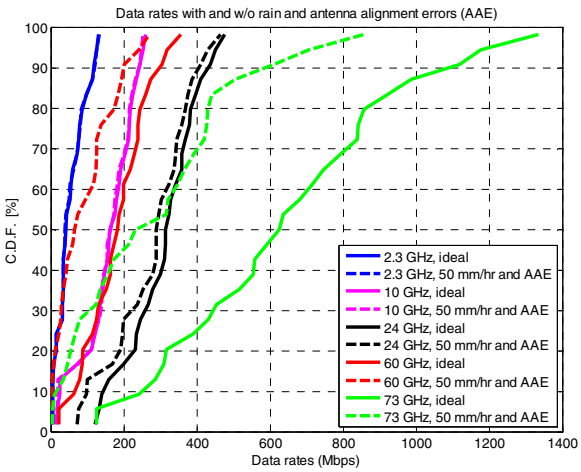


Figure 11: Data rates for the case study with 50 mm/hour rain and antenna alignment errors (AAE). The blue respective the pink curves are on top of each other.